Lab Notes

Editors
Thomas M. Moses | Shane F. McClure

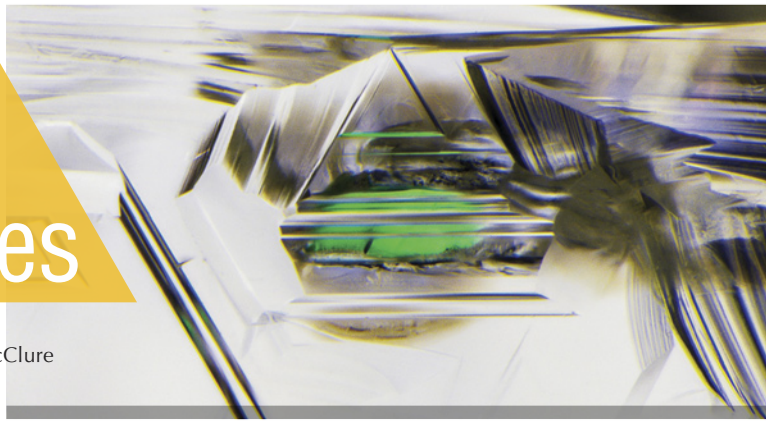

HPHT-Processed DIAMOND with Counterfeit GIA Inscription

In June 2021, GIA's Antwerp lab received a diamond treated by high pressure and high temperature (HPHT) that was falsely inscribed with a GIA report number referencing an untreated diamond originally graded by GIA in 2010. The diamond was submitted for Update service, in which a stone is matched to its previous report and regraded based on its current condition. Careful comparison of the diamond with its accompanying report number showed that the weight and grading parameters were very similar, but certain differences readily led to the conclusion that this was not the same stone.

The HPHT-processed diamond was a round brilliant weighing 1.497 ct and measuring 7.30–7.34 × 4.50 mm (figure 1), while the original diamond weighed slightly more (1.502 ct) and measured 7.29–7.34 × 4.56 mm. They had the same clarity (IF) and fluorescence (none) but different color grades (D for the original diamond, E for the HPHT-processed diamond).

Additional conclusive differences were detected when the newly submitted stone was further analyzed with advanced spectroscopic techniques. Whereas the diamond from 2010 was type Ia, the submission from 2021 tested as type IIa. Photoluminescence (PL) spectroscopy using various laser excitation wavelengths confirmed a natural origin, but with color enhancement by HPHT treatment.

Figure 1. Face-up view of the 1.497 ct, E-color HPHT-processed diamond submitted in 2021 for update service.

In addition to a clearly fraudulent inscription (not pictured), microscopic examination of the girdle revealed remnants of an original GIA inscription (figure 2). Based on this information, we found that this HPHT-processed stone had already been submitted to GIA in 2013 but was repolished afterward in an attempt to obscure the original inscription. Our records showed that in 2013, the diamond was also inscribed with "BELLATAIRE" (indicating HPHT treatment), but this information had been removed from the girdle and the remnants were even less visible than the original GIA inscription.

In addition to issuing a new report for this HPHT-treated diamond, GIA made the fraudulent inscription unreadable, according to standard procedure, and the stone was inscribed with "TREATED COLOR" (figure 3).

The Antwerp lab had recently reported a similar case of fraud, but that concerned a laboratory-grown diamond with a counterfeit inscription referencing a natural diamond (Sum-

Figure 2. Remnants of the original GIA report number could still be detected on the girdle of the diamond (in addition to the fraudulent inscription, which is not pictured).

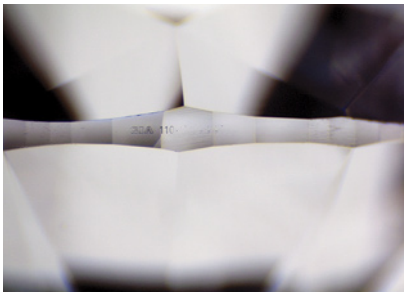

Figure 3. "TREATED COLOR" was inscribed on the girdle after spectroscopic analysis confirmed that the color of the stone was enhanced by HPHT treatment.

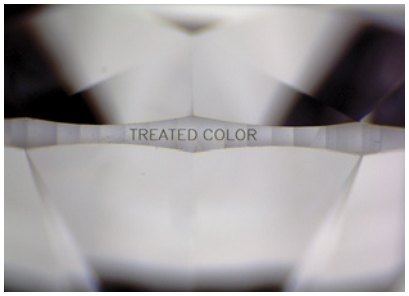

Editors' note: All items were written by staff members of GIA laboratories.

Gems & Gemology, Vol. 57, No. 3, pp. 258–267.

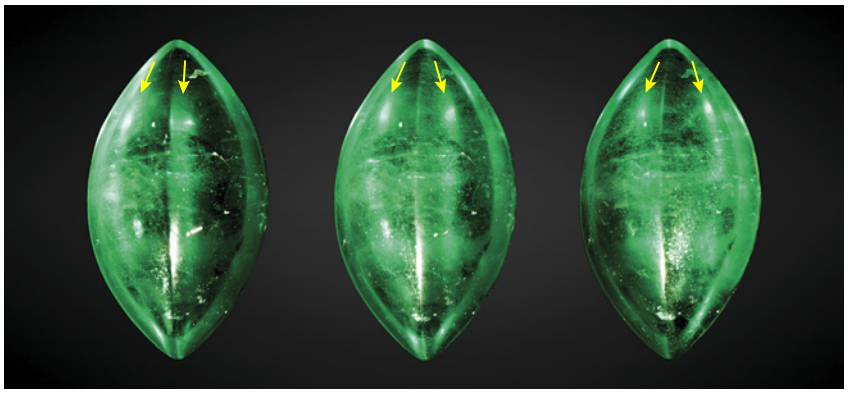

Figure 4. In this 1.93 ct double cat's-eye emerald, the chatoyant bands indicated by yellow arrows are observed from different angles of lighting.

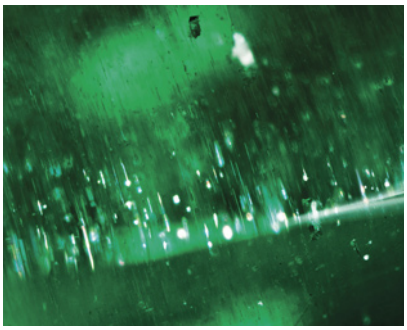

Figure 6. Numerous parallel needles and tubes causing chatoyancy. Field of view 1.75 mm.

mer 2021 Lab Notes, pp. 150–152). Both types of fraud are common in the marketplace and show the importance of careful verification of not only a diamond's growth method (natural versus laboratory-grown) but also its color origin.

Ellen Barrie, Sander Teuthof, and Sally Eaton-Magaña

EMERALD

A Unique Double Cat's-Eye Emerald

Chatoyancy is generally produced by light reflection from numerous parallel needle-like inclusions or fibrous structures when a stone is skillfully fashioned as a cabochon. Stones such as emerald, chrysoberyl, and scapolite are known for the cat's-eye effect (see Summer 2015 Gems News International, pp. 200–201). Recently GIA's Tokyo laboratory examined a unique green marquise double-cabochon stone, weighing 1.93 ct and measuring 11.88 × 6.68 × 4.79 mm, that offered a particularly interesting example of chatoyancy (figure 4).

This stone had a spot refractive index of 1.58 and a specific gravity of 2.74, and standard gemological properties indicated that it was emerald. The stone characteristically had a ridgeline and a high-dome structure (figure 5) containing numerous reflective oriented needles and tubes (figure 6) parallel to the width and perpendicular to the length of the stone. It was noteworthy that the light reflection from the inclusions created two distinct chatoyant bands along the length of the ridgeline (figure 4) under overhead light. These chatoyant bands were observed from different angles of lighting, as shown in figure 4. This double cat's-eye effect might result from a combination of face angles, inclusions, and the high-dome cabochon structure and ridgeline. Such an unusual cutting style could be responsible for creating this double cat's-eye (figure 7). The principle of double cat's-eye seen in this emerald is different from those of the dual-color double star effect rarely seen in ruby, sapphire, and quartz (e.g., K.

Figure 5. Emerald cabochon fashioned with a high-dome structure and ridgeline. The width of the stone is 6.68 mm.

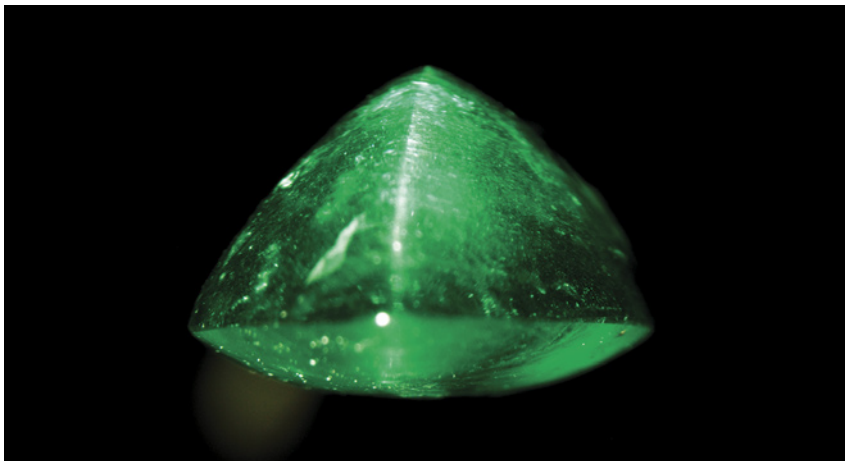

Figure 7. The double cat's-eye seen in the emerald results from the light reflection from oriented inclusions and the cutting style, as shown in this diagram.

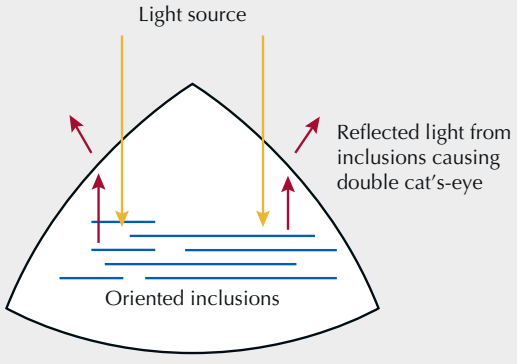

Figure 8. Eleven semitranslucent to opaque green and brown fossilized shells. Most of these specimens show clear shell outlines with green emerald grains.

Schmetzer et al., "Dual-color double stars in ruby, sapphire, and quartz: Cause and historical account," Summer 2015 *G&G*, pp. 112–143). This is a unique example of an unusual optical effect due to the cutting style and inclusion scene.

Makoto Miura

Fossilized Shell Consisting of Emerald

Fossilized shells can be replaced by various types of gemstones, such as quartz and chalcedony (Spring 2014 Gem News International, p. 77), opal (A. Cody and D. Cody, *The Opal Story: A Guidebook*, Melbourne, 2008), and demantoid garnet (Winter 2013 Gem News International, pp. 257–258). In rare cases, emerald may also participate in the petrification of the shell and form pseudomorphs.

Recently, the Hong Kong laboratory received 11 fossilized shells composed primarily of emerald, measuring 13.00 × 8.20 × 6.16 mm to 24.54 × 16.72 × 12.57 mm and weighing 3.22 to 20.63 ct (figure 8). Most of them preserved the distinctive gastropod shell outlines, with different degrees of weathering. Under magnification, numerous small light green to green anhedral emerald crystals contained very fine fluid inclusions associated with well-formed brassy pyrite grains (figure 9), which is one of the most common mineral inclusions in Colombian emeralds (S. Saeseaw et al., "Geographic origin determination of emerald," Winter 2019 *G&G*, pp. 614–646). An X-ray radiograph further revealed the spiral skeleton of the shell and scattered pyrite crystals (figure 10). The polycrystalline emerald was deposited evenly throughout the specimens, indicating complete replacement.

Fossilized gastropods were reported from the Matecaiia tunnel of the Gachala emerald mine in Colombia (P. Vuillet et al., "Les émeraudes de Gachalá, Colombie," *Le Regne Mineral*, No. 46, July/August 2002, pp. 5–18). Gachala is not a principal emerald mining district but can produce high-quality material. (D. Fortaleche et al., "The Colombian emerald industry: Winds of change," Fall 2017 *G&G*, pp. 332–358). It is located on the Lower Cretaceous fossiliferous sedimentary rocks of the Eastern Cordillera Basin (B. Horton et al., "Construction of the Eastern Cordillera of Colombia: Insights from the sedimentary record," in J. Gómez and D. Mateus-Zabala, Eds., *The Geology of Colombia*, Chap-

Figure 9. Well-formed pyrite is a common accessory mineral associated with Colombian emerald. Field of view 14 mm.

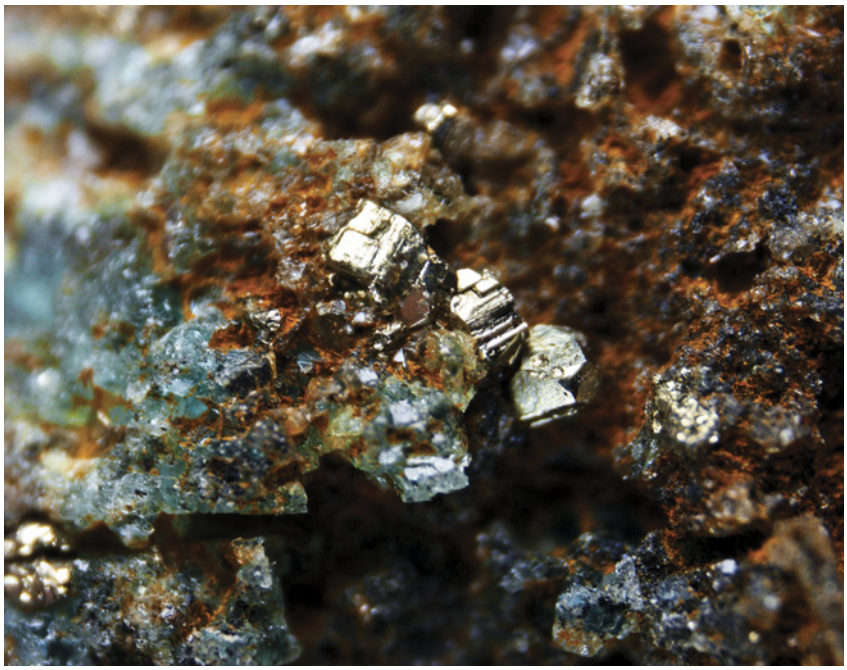

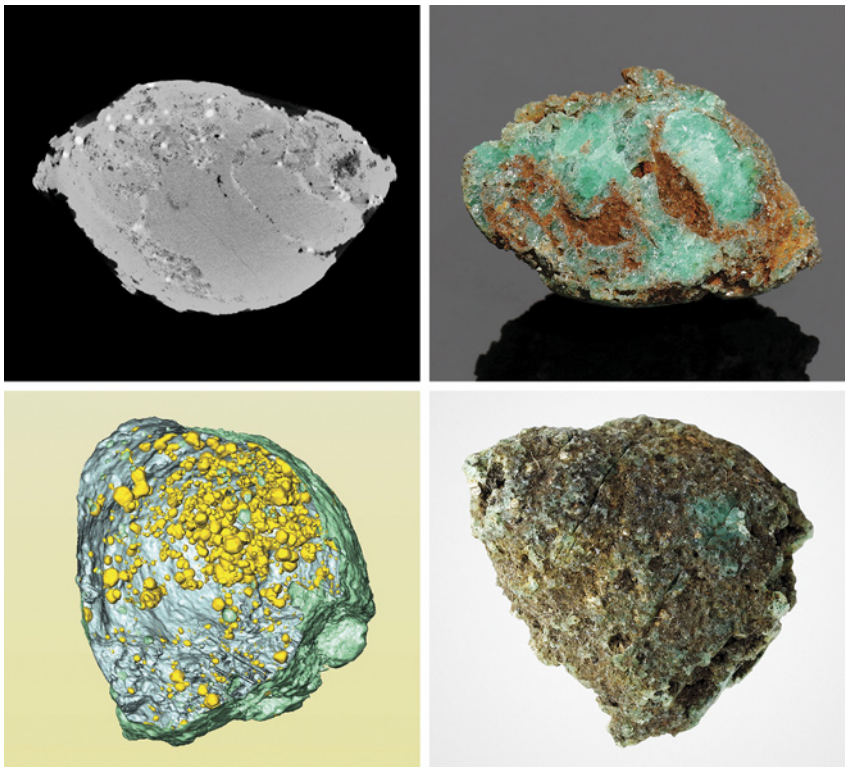

Figure 10. Clear shell structure and internal banding are shown in the X-ray radiograph (top left) of a fossilized shell measuring 22.06 × 14.85 × 10.32 mm and weighing 14.89 ct (top right). Scattered pyrite crystals (yellow in the colorized image on the bottom left) are deposited in a fossilized shell measuring 13.91 × 11.89 × 9.32 mm and weighing 5.07 ct (bottom right).

ter 3, Vol. 3, 2020, Servicio Geológico Colombiano, Publicaciones Geológicas Especiales 37, pp. 67–88), where pyrite and emerald crystallized during the circulation of hydrothermal mineralizing fluids in black shales (G. Giuliani and L. Groat, "Geology of corundum and emerald gem deposits," Winter 2019 *G&G*, pp. 464–489) and subsequently precipitated to form the fossilized shells.

Ching Yin Sin and Xiaodan Jia

GLASS Imitation of Star Sapphire

The market for sapphire simulants and synthetics is plentiful, as sapphire is likely the most popular of all colored stones. The high cost of natural, gem-quality sapphire means it is not obtainable for much of the world's population. This has opened the doors of creativity to produce blue stones with high luster resembling the natural material. Recently, the author obtained a parcel of blue cabochons with an unusual star pattern resembling star sapphire (figure 11). After a series of tests were performed, the material was identified as manufactured glass.

Gemological investigation revealed an average specific gravity of 2.46 and a refractive index of 1.40. The cabochons were inert to long-wave ultraviolet radiation but exhibited strong chalky blue fluorescence under short-wave ultraviolet radiation. Observation under a microscope revealed gas bubbles shallow to the surface within the blue regions of the stones and small conchoidal fractures along the girdles. One cabochon was cut in half vertically for further scientific investigation (figure 12). This cross section uncovered a large core of white glass raised to the surface of the dome in a star pattern. Flow lines were also visible within the white glass core. Finally, a thin layer of blue

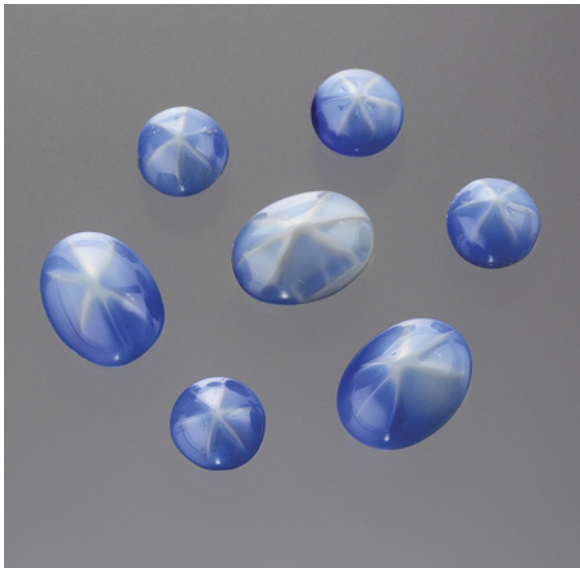

Figure 11. Glass cabochons with weights ranging from 0.47 to 1.29 ct were obtained by the author. The stones displayed white six-ray stars across their domes, resembling star sapphire.

glass around the perimeter of the cabochon was seen in the cross section, creating the bodycolor of the stone (again, see figure 12).

Asterism is an optical phenomenon that can be defined as a star-shaped concentration of reflected or refracted light from inclusions within a gemstone cut en cabochon. Genuine asterism is also mobile if the stone and/or light source is moved. These

Figure 12. A vertical cross section of the glass cabochon showcases the internal structure and diagnostic flow lines imitating star sapphire.

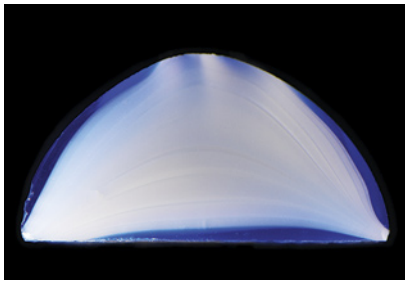

Figure 13. These 10 CVD-grown diamonds submitted to the New York laboratory were fairly large (2.24 ct to 5.90 ct) with high color grades (D to F) and excellent clarity (VVS_2 to VS_1).

glass imitation star sapphires, however, do not exhibit genuine asterism, as their stars were simply molded into shape and are fixed in place.

Glass imitations span the gamut of gemstones. Faceted transparent colorless glass is one of the oldest and simplest diamond simulants. Glass beads coated with pearlescent paint are a common pearl imitation, and colored glass of various opacities is capable of imitating almost any colored gemstone. Recent *G&G* articles on colored stone imitations include "Artificial glass imitating a Paraíba tourmaline" (Winter 2020 Lab Notes, pp. 518–520), "Greenish blue glass imitating gem silica" (Summer 2020 Gem News International, pp. 314–315), and "Glass bangles" imitating jadeite and nephrite (Spring 2019 Lab Notes, pp. 93–94).

Britni LeCroy

LABORATORY-GROWN DIAMONDS

New CVD Material Submitted for Analysis

Since the introduction of its new digital Laboratory-Grown Diamond service, GIA has recently seen a vast increase in the number of diamonds grown by chemical vapor deposition (CVD). These are often large and of exceptional clarity. The New York laboratory recently examined a batch of 10 large, high-quality CVD-grown diamonds from a single client, Shanghai Zhengshi Technology. The diamonds ranged from 2.24 ct to 5.90 ct and came in a variety of fancy shapes, as well as the standard round brilliant cut. All of them had high color grades, ranging from D to F, and excellent clarity, with grades between VVS_2 and VS_1 (figure 13).

The diamonds were all identified as type IIa using Fourier-transform infrared (FTIR) spectroscopy, with the 3123 cm^{-1} peak that is attributed to most as-grown CVD synthetics and the 3017 cm^{-1} peak that can be found in treated CVD synthetics both notably absent from their spectra. PL spectroscopy using a 514 nm laser revealed SiV (737 nm), NV^- (637 nm), and NV^0 (575 nm) centers in all of the diamonds. Also observed was the 596/597 nm doublet, a feature commonly seen in as-grown CVD diamond indicating no treatment was applied (figure 14) (S. Odake, "Melee diamonds: Metal defects and treated color," Fall 2018 *G&G*, p. 304).

Figure 14. PL spectrum showing the 596/597 nm doublet observed in an as-grown CVD diamond.

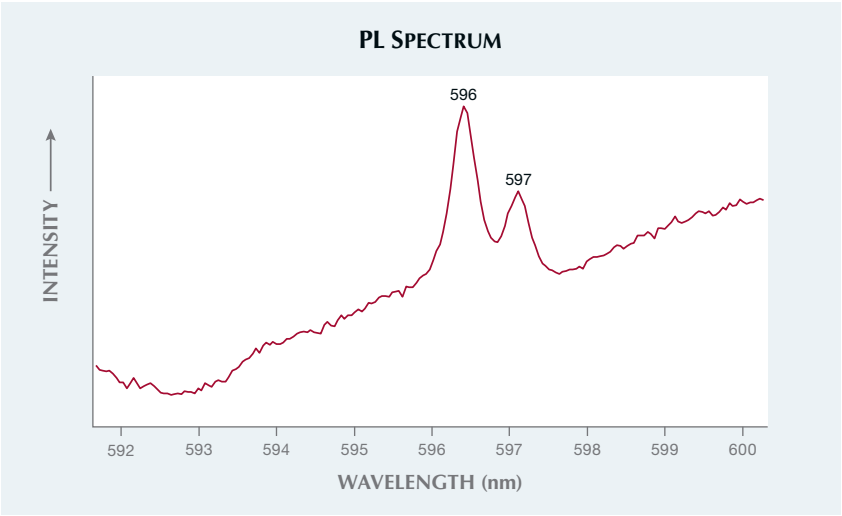

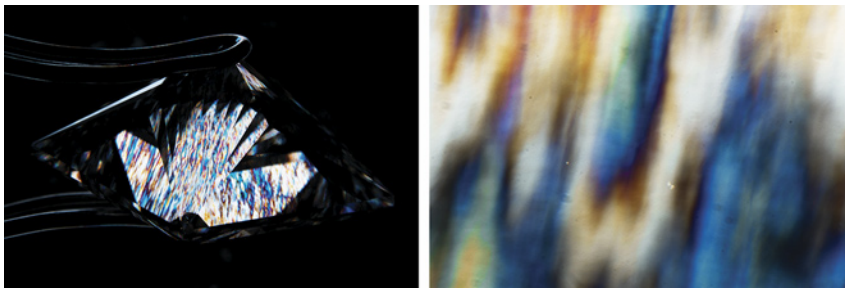

Figure 15. Each CVD-grown diamond showed a strong birefringence pattern displaying many interference colors. The pattern is not disrupted by the presence of pinpoint inclusions in the diamonds. Field of view 19.27 mm (left) and 1.26 mm (right).

The diamonds showed strong birefringence when viewed under cross-polarized light, exhibiting both low and high interference colors (figure 15). DiamondView imaging revealed mostly blue, purple, or pink fluorescence, with blue-violet dislocations that were clearly observed in all of the diamonds tested. More notable was the absence of the striations commonly seen in CVD diamonds, which indicate start-stop growth and changing growth conditions (figure 16). The absence of striations implies that these diamonds might have been grown in one continuous step—the fact that the dislocations appear to be homogenous and uninterrupted supports this theory.

This group of lab-grown diamonds possessed high clarity and high color for as-grown material, demonstrating the potential for large lab-grown diamonds to make large inroads in the gem diamond market. With continuing improvements to growth technology, lab-grown diamond identification faces many challenges. While large batches of CVD synthetics from different manufacturers have been documented by GIA in the past (e.g., W. Wang et al., "CVD synthetic diamonds from Gemesis Corp.," Summer 2012 *G&G*, pp. 80–97), this set offers insight into potential new CVD growth conditions for CVD synthetic diamonds.

Elina Myagkaya and Paul Johnson

Laboratory-Grown Diamond with Internal Laser Markings

With the recent influx of laboratory-grown diamonds into the market and to aid consumer awareness of diamond origin, manufacturers are often marking their laboratory-created diamonds using internal inscriptions. The New York laboratory recently examined a 2.44 ct pear-shaped CVD (chemical vapor deposition) grown diamond with unusual internal spiral markings (figure 17).

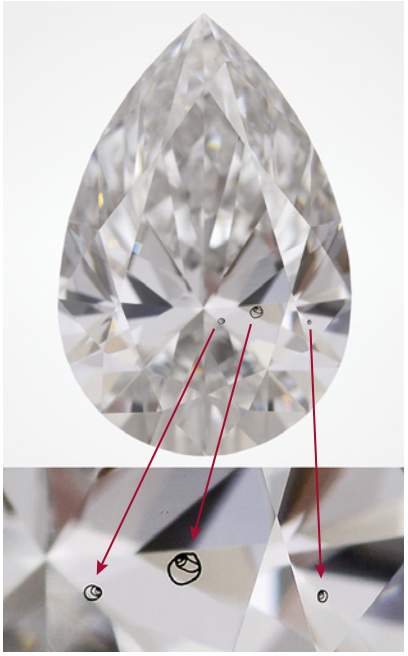

Figure 17. The 2.44 ct pear-cut CVD-grown diamond with internal spiral markings.

The three spiral markings were black and all in the same plane (i.e., at the same depth). The line thickness of these markings was about 40 microns (figure 18), whereas laser inscriptions are generally less than 20 microns. It was suspected that these markings were created by accidental laser dam-

Figure 16. DiamondView imaging revealed homogenous, unbroken dislocations without the distinct banding that is common in CVD-grown diamonds.

Figure 18. Micro image of the largest spiral marking; the line thickness is 40 microns.

Figure 19. These four non-nacreous pink and light pink pearls submitted for identification weighed (left to right) 1.30, 2.88, 4.41, and 5.88 ct.

age rather than laser inscription. Raman mapping of the surface above the markings revealed a much broader diamond Raman peak compared to the rest of the crystal. This is the result of laser damage to the crystal lattice. Further Raman mapping using confocal settings identified a graphite peak at about 1620 cm^{-1}. This offered proof that a laser, graphitizing the diamond, had created the markings.

The "inclusions" likely resulted from the laser marking the surface; this is done to provide a template to guide the polisher in producing the final shape. The intent would have been to score the surface; however, the laser appeared to have been inadvertently focused below the surface, resulting in the unusual internal markings.

As the markings are internal and graphitized, they are considered clarity features. The clarity grade was determined to be SI_1, followed by a report comment stating, "Clarity grade is based on manufacturing remnants that are not shown."

Paul Johnson, Stephanie Persaud, and Cori Bulgrin

Dyed Non-Nacreous PEARLS

Recently, 90 items purported to be pearls were submitted to GIA's Bangkok laboratory for identification. While the majority were confirmed to be natural pearls, four samples warranted further study. Each of these four samples exhibited a non-nacreous surface, and on first impression they appeared to be conch pearls owing to their pink and light pink coloration. Their measurements ranged from 6.53 × 5.11 × 4.92 mm to 10.64 × 10.46 × 7.28 mm, and they weighed 1.30, 2.88, 4.41, and 5.88 ct, respectively (figure 19).

Observation through a 10× loupe and a microscope revealed that the samples were non-nacreous pearls. However, it was also readily apparent that the colors had been modified and were not natural. The 1.30 ct pearl exhibited the flame-like structure routinely observed in pearls such as conch, but the obvious red dye visible over the entire surface made it difficult to determine whether the flame structure was really present (figure 20A). The 2.88 ct pearl displayed a subtle flame structure, and some pink dye was visible on the surface and within many surface blemishes (figure 20B). Some surface areas of the 4.41 ct pearl showed the original bodycolor (figure 20C), but much of the surface showed the same dye features seen in the previous two pearls. Finally, the 5.88 ct pearl exhibited a nice flame pattern throughout, with some surface areas on the base and circumference modified by working (*The Pearl Book*, CIBJO Pearl Commission, 2020; N. Nilpetploy et al., "A study on improving the surface appearance of low-quality *Pinctada maxima* bead cultured pearls," *GIA Research News*, March 24, 2021).

The color origin of this pearl was a little more challenging to identify because most areas were a lighter color, and as a result, the color modification evidence was harder to see with the unaided eye. However, magnification revealed pink dye concentrations within cracks on the base and in some surface-reaching structural features (figure 20D). Real-time microradiography (RTX) revealed a variety of structures within the pearls. The organic-rich and void features ob-

Figure 20. A: Red dye visible within surface-reaching features of the 1.30 ct pearl; field of view 3.60 mm. B: Red dye concentrated in and around surface-reaching features of the 2.88 ct pearl; field of view 2.88 mm. C: An underlying white area where the red dye did not cause discoloration of the 4.41 ct pearl. Flame structure is evident in the white area; field of view 7.20 mm. D: Clear flame structure with areas of pink dye concentrated in the surface features of the 5.88 ct pearl; field of view 7.20 mm.

served could be interpreted as characteristic of some non-bead cultured pearls. While they may be considered suspect, similar features have been observed in natural non-nacreous pearls (E. Fritsch and E.B. Misiorowski, "The history and gemology of Queen conch 'pearls'," Winter 1987 *G&G*, pp. 208–221; S. Singbamroong et al., "Observations on natural non-nacreous pearls reportedly from Tridacna (clam) species)," *34th International Gemmological Conference*, Vilnius, Lithuania, 2015; Summer 2018 Lab Notes, pp. 211–212). To date, there have been no reports of any *commercially produced* non-nacreous cultured pearls in the market. Thus, based on surface observations and their internal structures, they were identified as treated-color natural non-nacreous pearls.

Further examination under long-wave ultraviolet radiation showed a weak to moderate red reaction over the colored areas, while the white area on the 4.41 ct pearl and the lighter-colored areas on the 5.88 ct pearl exhibited bluish reactions of moderate to strong intensity. Ultraviolet-visible (UV-Vis) reflectance spectra revealed absorption features expected for pink pearls in the visible range, but the absorption patterns differed from those typical of naturally colored conch pearls. Raman spectra collected using a 514 nm laser revealed peaks (doublet) related to the vibration modes of aragonite at 702 and 705 cm^{-1}. All of the pearls showed additional weak peaks at 485, 640, and 827 cm^{-1} and less-defined features between 1000 and 1700 cm^{-1}. However, none were associated with the polyenic peaks observed in most naturally colored non-nacreous pearls (Summer 2017 Lab Notes, pp. 230–231; Summer 2018 Lab Notes, pp. 211–212). The photoluminescence spectra also differed from those expected for naturally colored pink conch pearls and lacked the obvious polyenic peaks routinely observed in such pearls (figure 21).

Surface observation using the loupe and microscope combined with the results obtained from advanced analyses on the colored surface areas led us to conclude that the colors of the four pearls had been modified. While this is not so surprising when it comes to nacreous pearls, it is, from the author's experience, more unusual to encounter color-modified natural non-nacreous pearls. Since these sam-

Figure 21. Photoluminescence spectra of the four pearls together with the spectrum of a pink conch pearl from GIA's reference database. The spectra of the treated pearls differ from that of the conch pearl, which shows a series of very clear polyenic peaks. These peaks are characteristic of many naturally colored porcelaneous pearls.

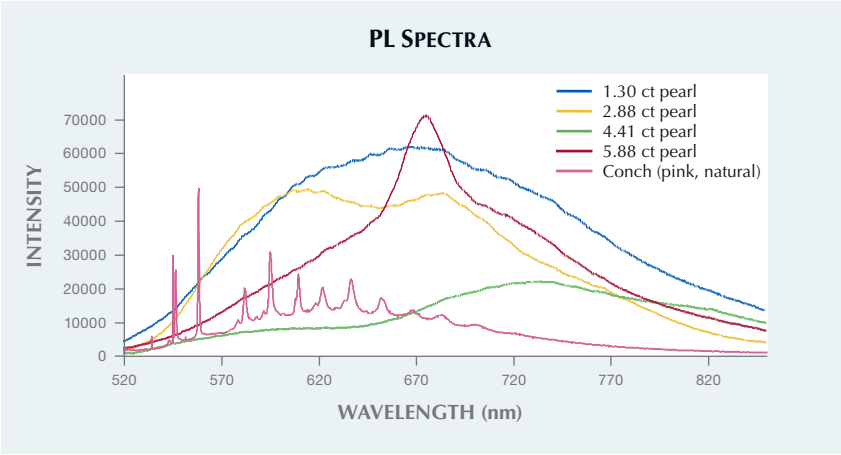

ples appeared visually similar to conch pearls, we can speculate that the original white or lightly colored pearls were dyed pink to imitate those produced by the Queen conch mollusk (*Lobatus gigas*, formerly known as *Strombus gigas*). This would make sense based on consumer demand in the market. However, the exact reason for treating these particular samples is unknown.

Areeya Manustrong

ZIRCON with Unusual Color-Change Behavior

The Carlsbad laboratory recently had the chance to examine a 4.60 ct cushion-cut zircon with truly unusual color behavior. Standard gemological testing confirmed that the stone's properties were consistent with zircon: an over-the-limit RI, an SG of 4.72, weak yellow fluorescence in short-wave UV and no fluorescence in long-wave UV, and a typical uranium-related pattern in the spectroscope with a prominent sharp peak at 653 nm. The zircon's color was green using a standard white light fluorescent illuminant with a color temperature of 5500 K (figure 22). The stone's color was also checked using a standard incandescent illuminant, but there was no discernible difference from the cool fluorescent illuminant (table 1). However, the color of the zircon was markedly different using white light LEDs with variable color temperature from 2700 K (warm) to 6500 K (cool), where the color went from grayish purple in cool LED light to green in warm LED light (figure 23). Notably, the color observed in the cool LED light was quite similar to the color seen when the stone was taken outside and observed in diffused daylight.

The discrepancy between the colors seen using the cool fluorescent illuminant (green) and either daylight or the cool LED illuminant (grayish purple) can be understood by studying the absorption spectrum of the zircon compared to the emission spectrum of the cool fluorescent bulb (figure 24).

TABLE 1. Color behavior of the color-change zircon under different illuminants.

Illuminant	Observed color
Incandescent (2700 K)	Green
Daylight (overcast afternoon, Carlsbad, Calif.)	Grayish purple
Cool fluorescent (6500 K)	Green
Warm LED (2700 K)	Green
Cool LED (6500 K)	Grayish purple

Figure 22. The color of the 4.60 ct zircon is shown in standard cool fluorescent illumination (left) and in warm (2700 K) LED illumination (right). There was little difference in bodycolor when viewed under the two light sources.

The perception of cool white light output from the fluorescent bulb is achieved with two relatively sharp emission bands at about 435 nm and 545 nm, which is in contrast to the much smoother broad-band emission pattern of true daylight. One of the sharp emission bands in the fluorescent illuminant overlaps significantly with sharp absorption bands in the

Figure 23. The color of the 4.60 ct zircon is shown in LED illumination with cool white light at 6500 K (left) and in warm white light at 2700 K (right).

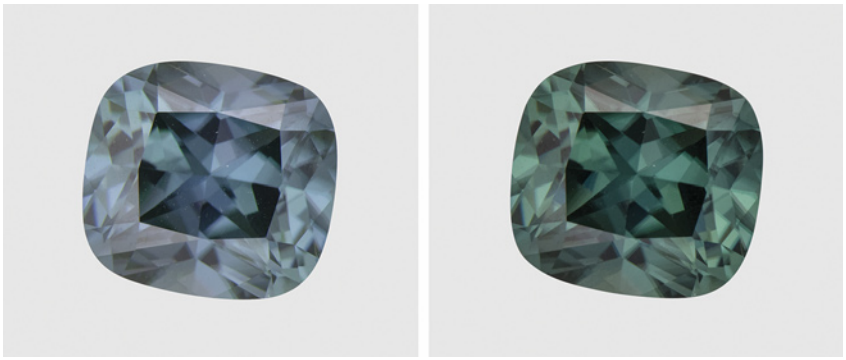

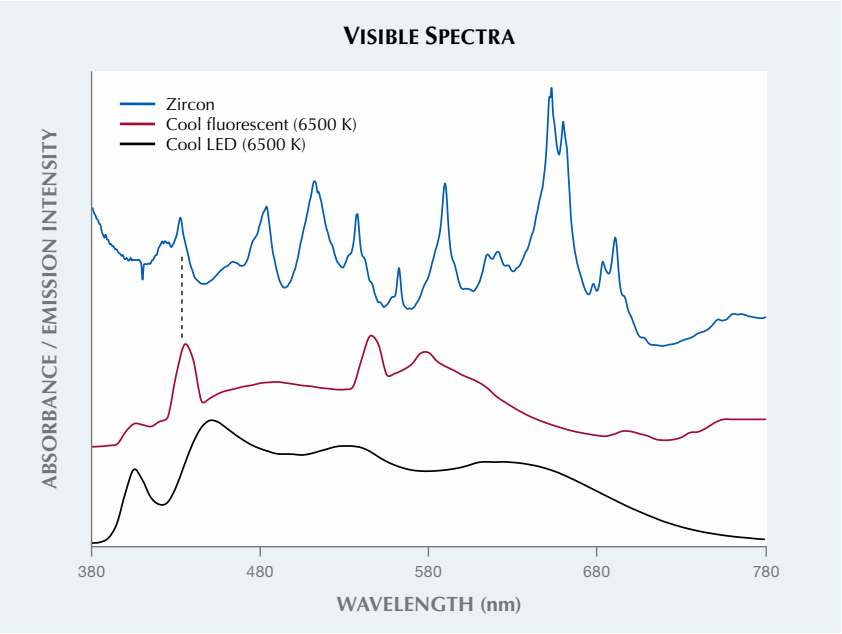

Figure 24. The visible absorption spectrum of the color-change zircon (top) compared to the emission spectrum of a standard cool (6500 K) fluorescent illuminant showing the overlap of sharp emission bands from the fluorescent light and sharp absorption bands in the absorption spectrum (dashed line). Also shown is the emission spectrum of the cool (6500 K) LED used in the lab for color grading at GIA.

zircon at 424 and 433 nm. The fact that a significant portion of the blue emission from the fluorescent bulb is selectively absorbed by the zircon skews its color away from the blue color that ought to be observed in true daylight. This blue can also be observed using cool LEDs, which tend to have smoother broad emission patterns more closely resembling blackbody radiation patterns of true daylight and incandescent light. This unusual color-change behavior is only expected in gems with sharp absorption bands, likely related to either rare earth or actinide elements. Of particular note, these color-change zircons are occasionally recovered from the gem mining areas around Mogok, Myanmar. For these gems, LEDs should provide a more reliable color grading illumination environment than fluorescent light sources.

Aaron Palke

PHOTO CREDITS
Ellen Barrie—1, 2, 3; Makoto Miura—4, 5, 6; Johnny Leung—8, 9, 10; Cheryl Wing Wai Au—10 (top); Ching Yin Sin—9, 10 (bottom); Emiko Yazawa—10 (bottom); Jessa Rizzo—11; Nathan Renfro—12; Sood Oil (Judy) Chia—13; A'Dhi Lall—15; Elina Myagkaya—15, 16; Jian Xin Liao—17; Paul Johnson—18; Lhapsin Nillapat—19; Kwanreun Lawanwong—20; Robert Weldon—22, 23